

## Mesoporous Silica Nanoparticles Supported Atomically Precise Palladium Nanoclusters Catalyzed Aerobic Oxidation of Alcohols in Water

Taiping Gao\*, Xiaolin Ma, Xin Li, Qiang Xu and Yubao Wang\*  
School of Chemistry and Materials Science, Ludong University, Yantai 264025, P.R. China  
[gaotp@ldu.edu.cn](mailto:gaotp@ldu.edu.cn)\*

(Received on 29<sup>th</sup> May 2020, accepted in revised form 15<sup>th</sup> November 2020)

**Summary:** The first mesoporous silica nanoparticles (MSNs) supported atomically precise palladium nanoclusters catalyzed alcohol oxidation reactions in water have been achieved. The catalysts were synthesized with simple impregnation method and well characterized by TEM, FT-IR, XPS and diffuse reflectance optical spectrum and the results proved that the Pd nanoclusters immobilized into the pores of MSNs. The as-prepared catalyst shows excellent activity for the alcohol oxidation reactions with high yield under extremely mild aqueous conditions utilizing 1 atmosphere of molecular oxygen as sole oxidant. The features of clean system, gram-scale oxidation and easy recovery catalyst make this method cost effectively and environmentally benign.

**Keywords:** Atomically precise Palladium nanoclusters, Heterogeneous catalysis, Alcohol oxidations, Green synthesis, Aqueous media.

### Introduction

Due to its abundance, cost-efficiency, nontoxicity, and sustainability, water is widely recognized as the natural solvent for organic transformations [1]. Life most likely emerged in an aqueous surrounding, many biochemical reactions catalyzed by enzyme occur in this medium. As traditional organic reactions typically require anhydrous conditions, much effort is needed to construct such conditions. So, the operating procedure of organic reactions will be greatly simplified using water as a reaction medium. Selective oxidation of alcohols to aldehydes is one of the fundamental importance and widely used transformations in synthetic organic chemistry [2]. Metallic catalysts, such as Au [3], Pd [4], Pt [5], Cu [6] and Ru [7], have been commonly used for heterogeneous or homogeneous catalysis in this reaction with organic solvents. However, organic solvents often suffer from severe problems including cost, toxicity and environmental pollution, which is against the principles of green chemistry [8]. Therefore, highly efficient and environmentally benign transformation of alcohol into aldehyde is still a desirable, yet challenging task.

As one of the most promising branches of nanoscience and nanotechnology, Atomically precise nanoclusters (APNCs), which exhibit specific physicochemical properties that have not been observed in the corresponding nanoparticles and bulk materials, have attracted significant attentions during

the past 10 years. [9] Owing to its high surface-to-volume ratio, monodispersity and the unique core-shell structure, APNCs show distinct catalytic activity in selective oxidations [10], reductions [11] and carbon-carbon coupling reactions [12]. Furthermore, nanocluster with exact number of atoms and determined crystal structure make it possible to correlate the catalytic performance with their atomic level structure and then study the mechanisms, which enable it have huge advantages over the uncertain surface structure of traditional metal nanoparticles [13]. In 2012, Tsukuda and co-workers reported the Au<sub>25</sub> and single-palladium-doped Pd<sub>1</sub>Au<sub>24</sub> nanoclusters supported on multiwalled carbon nanotubes catalyzed benzyl alcohols oxidation in water using O<sub>2</sub> as the oxidizing agent [14]. Unfortunately, the mixture of benzaldehyde, benzoic acid and benzyl benzoate are produced under the optimum conditions. In 2017, Zhu et al. synthesized and well characterized [Pd<sub>3</sub>Cl(PPh<sub>2</sub>)<sub>2</sub>(PPh<sub>3</sub>)<sub>3</sub>]<sup>+</sup>[SbF<sub>6</sub>]<sup>-</sup> (abbreviated Pd<sub>3</sub>Cl) nanocluster, and investigated the catalytic performance of free Pd<sub>3</sub>Cl in the Suzuki–Miyaura C–C cross coupling reactions of aryl bromides and arylboronic acids (Scheme 1a) [15]. Recently, the same group reported titanate nanotubes supported Pd<sub>3</sub>Cl nanoclusters catalyzed the oxidation of aromatic alcohols in toluene (Scheme 1b) [16]. Despite this progress, the development of efficient, safe and environmental benign transformation catalyzed by ultrasmall Pd nanocluster is still valuable and practicable. So we developed and herein report the Mesoporous Silica

\*To whom all correspondence should be addressed.

Nanoparticles (MSNs) supported Pd<sub>3</sub>Cl nanoclusters catalysts for the selective oxidation of various alcohols to aldehydes using O<sub>2</sub> as terminal oxidant and water as solvent (Scheme 1c).

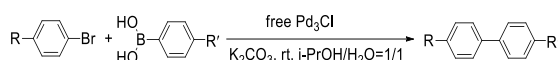
## Experimental

### Materials

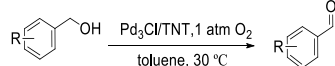
All reagents used in the experiment were analytical grade and used without further purification. Sodium borohydride (NaBH<sub>4</sub>), Triphenylphosphine (PPh<sub>3</sub>) and tetraethylorthosilicate (TEOS) were purchased from Sinopharm Chemical Reagent Beijing Co., Ltd (Beijing, China). cetyl-trimethylammonium tosylate (CTATos) and triethanolamine (TEAH<sub>3</sub>) were supplied by J&K Scientific Ltd (Beijing, China). PdCl<sub>2</sub> were from Beijing Chemicals Co. Ltd. (Beijing, China). Deionized water in experiments was prepared using Millipore purification system (Bedford, Ma, USA).

### Previous works:

a) free Pd<sub>3</sub>Cl as catalyst

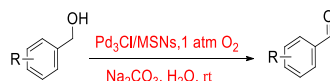


b) titanate nanotubes supported Pd<sub>3</sub>Cl cluster as catalyst



### This work:

c) MSNs supported Pd<sub>3</sub>Cl nanocluster for the selective oxidation of alcohol with water as solvent.



Scheme-1: The catalytic performance of Pd<sub>3</sub>Cl.

### Characterization

Flash chromatography was carried out using silica gel (200-300 mesh). The Ultraviolet visible (UV-vis) absorption spectra were recorded on a UV-2550 UV spectrophotometer (Shimadzu, Japan) at room temperature. Fourier transform infrared (FTIR) analysis was characterized on a Magna 750 FTIR spectrophotometer in the 400–4000 cm<sup>-1</sup> range (Thermo Nicolet Corporation, USA). Transmission electron microscope (TEM) images were gained with a JEM-100SX (Japan Electronics, Japan) transmission electron microscope under an acceleration voltage of 200kV. The matrix-assisted laser desorption ionization mass

spectrometry (MALDI-MS) was performed on Agilent and Bruker instruments. *trans*-2-[3-(4-*tert*-Butyl-phenyl)-2-methyl-2-propenylidene]malononitrile (DCTB) was used as the matrix. The Pd<sub>3</sub>Cl loading of the supported catalyst was determined by inductively coupled plasma characterization (ICPE, Shimadzu, Japan).

### Synthesis

#### General procedure for the preparation of the Pd<sub>3</sub>Cl nanoclusters.

The synthesis and separation procedure of Pd<sub>3</sub>Cl nanocluster was described in previous work. Briefly, PdCl<sub>2</sub> (1.42 g, 8 mmol) was dissolved in hydrochloric acid (1.33 ml, 16 mmol), and then the solution was diluted to 10 ml with deionized water. 0.6 ml of the above solution (0.48 mmol) was added into 10 ml tetrahydrofuran (THF), followed by the addition of PPh<sub>3</sub> (0.313 g, 1.2 mmol). After vigorous stirring for 10 min, NaBH<sub>4</sub> (0.08 g, 2.1 mmol) dissolved in 5 ml of ethanol was added. A strong H<sub>2</sub> flow was formed and the reaction solution turned dark immediately. The reaction was kept under vigorous stirring for 2 hours. Then centrifugation was performed to remove excess PPh<sub>3</sub>, and the remaining solution was evaporated to dryness in vacuo on rotary evaporator. Then the solid was washed with water and hexane several times to remove excess salt and other side products.

#### General procedure for the preparation of the MSNs.

A mixture of 1.92 g of CTATos, 3.47 g of TEAH<sub>3</sub> and 100 mL of deionized water was stirred at 80 °C for 1 hour, and then 14.58 g of TEOS was quickly added into the surfactant solution. The mixture was stirred at 80 °C for another 2 hours. The synthesized MSNs were centrifuged, washed with water and ethanol, dried and calcined at 550 °C for 6 hours.

#### General procedure for the preparation of the Pd<sub>3</sub>Cl/MSNs.

The Pd<sub>3</sub>Cl/MSNs catalysts were prepared as follows: typically, to MSNs powders (200 mg) was added dichloromethane (DCM) (10 ml) and the resulting suspension was sonicated for 5 minutes. Under vigorously stirring, 15 mg Pd<sub>3</sub>Cl, which had been dissolved in 10 ml DCM, was added to the above suspension dropwise. After stirring for 12 hours at room temperature, the supported Pd<sub>3</sub>Cl/MSNs catalyst was collected by centrifugation and drying. The catalyst was then annealed at 100 °C

for 2 hours in vacuum oven before the characterization and catalytic tests

*General procedure for the alcohol oxidation reaction.*

To a 10 ml Schlenk tube equipped with a stir bar, alcohol (0.2 mmol), Pd<sub>3</sub>Cl/MSNs (15 mg), H<sub>2</sub>O (1 ml) and base (0.3 mmol) was added successively. Then the tube was sealed by a rubber stopper and the air was replaced by O<sub>2</sub> three times. The reaction mixture was stirred 24 hours under O<sub>2</sub> atmosphere at room temperature. After the alcohol was complete consumption, the mixture was purified by flash chromatography (silica gel, mixtures of petroleum/ethyl acetate) to afford the pure product.

## Results and Discussion

Scheme 2 outlines the synthetic strategy of Pd<sub>3</sub>Cl/MSNs catalysts. First, the Pd<sub>3</sub>Cl nanoclusters were prepared by reducing of Pd<sup>2+</sup> with NaBH<sub>4</sub> in the presence of PPh<sub>3</sub>. The UV-vis absorption spectrum of the as-prepared Pd<sub>3</sub>Cl nanoclusters, dissolved in dichloromethane, shows a main peak at 418 nm and a shoulder peak at 485 nm (Figure 1A). MALDI-MS analysis of the as-prepared Pd<sub>3</sub>Cl clusters with positive model in figure 1(B) shows mass peak at m/z = 1511.9 (assigned to molecular ion peak of [Pd<sub>3</sub>Cl(PPh<sub>3</sub>)<sub>3</sub>(PPh<sub>2</sub>)<sub>2</sub>]<sup>+</sup>, theoretical molecular weight: 1511.9). Both the UV-vis absorption spectra and MALDI-MS analysis undoubtedly confirm that the Pd<sub>3</sub>Cl nano clusters were successfully obtained.

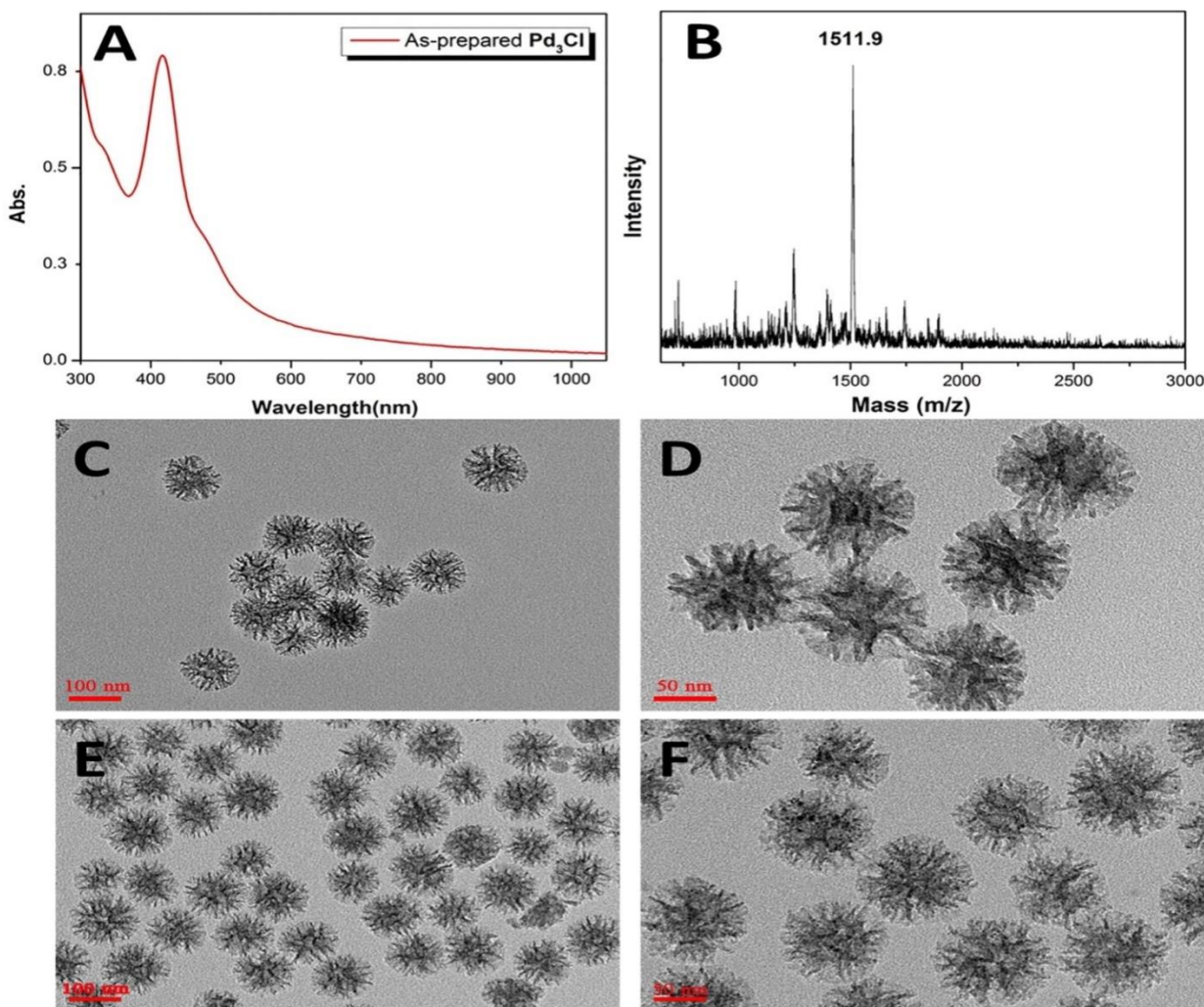
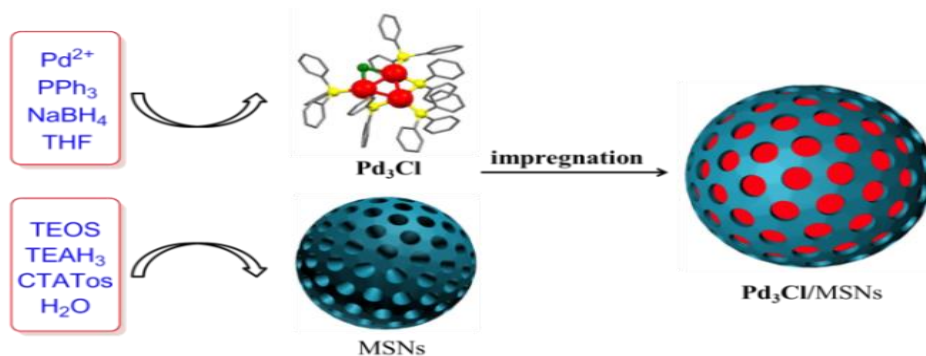
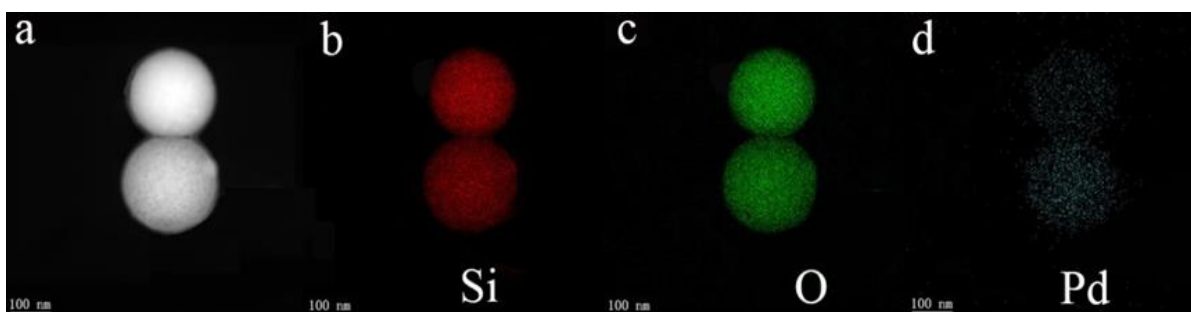


Fig. 1: (A) UV-vis spectrum of as-prepared Pd<sub>3</sub>Cl nanoclusters (in DCM), (B) Positive mode MALDI mass spectrum of Pd<sub>3</sub>Cl nanoclusters, (C) and (D) TEM images of MSNs, (E) and (F) TEM images of Pd<sub>3</sub>Cl/MSNs catalysts.

Scheme-2. The synthetic strategy of Pd<sub>3</sub>Cl/MSNs.Fig. 2: TEM image of Pd<sub>3</sub>Cl/MSNs (a), EDX mapping analysis of Si (b), O (c) and Pd (d).

Then the MSNs were synthesized with a soft-templating method using cetyltrimethylammonium as the templating surfactant, TEOS as silicon source and TEAH<sub>3</sub> as the mineralizing agent. The uniform morphology with average particle size ~100 nm of MSNs can be easily observed from the TEM image (Figures 1C and 1D). Benefiting from its rough surfaces and regular stellate-like porous structure, MSNs have large specific surface area and therefore emerged as an excellent supports. The Pd<sub>3</sub>Cl nanoclusters were immobilized in the MSNs with a simple impregnation method. Owing to the abundant porous structure of MSNs and the ultrasmall size of Pd<sub>3</sub>Cl nanoclusters, the Pd<sub>3</sub>Cl nanoclusters are deposited into the pores of MSNs (Figures 1E and 1F). To confirm the Pd nanoclusters after loaded on the MSNs are well dispersed, the energy dispersive X-ray spectroscopy (EDX) mapping analysis of Si, O, and Pd was conducted and shown in Figure 2. The results demonstrate that the Pd element is distributed homogeneously throughout the whole MSNs. In addition, ICP-MS analysis shows that the Pd content of the Pd<sub>3</sub>Cl/MSNs catalyst is 1.2 wt. %.

To confirm the Pd<sub>3</sub>Cl after immobilized on the

MSN support are intact, we performed the diffuse reflectance optical of the catalysts. As shown in figure 3, the MSNs have no distinct absorption peak in diffuse reflectance optical spectra from 200 nm-1000 nm (black line). The unsupported Pd<sub>3</sub>Cl nanoclusters shows absorption peak at 418 nm and 484 nm (Figure 3A, red line), which is good agreement with the optical spectrum of free Pd<sub>3</sub>Cl in DCM in Figure 1A. The peak at 418 nm and 484 nm also can be clearly found after immobilized on the MSNs (Figure 3A, blue line). These results confirmed that the Pd<sub>3</sub>Cl nanoclusters after immobilized on the MSNs are intact. Finally, the free Pd<sub>3</sub>Cl, MSNs and Pd<sub>3</sub>Cl/MSNs were analyzed by FT-IR and the results are shown in figure 3B. A strong absorption at 1439 cm<sup>-1</sup> was observed in Pd<sub>3</sub>Cl owing to the stretching vibration of Ph-P bond, which is the characteristic absorption peak of triphenylphosphine group. After loading on the MSNs, the absorption peak was still observed (Figure 3B, red line). The peaks at 2940 cm<sup>-1</sup> and 693 cm<sup>-1</sup> assigned to stretching vibration and bending vibration of C-H bond, respectively. Altogether, the Pd<sub>3</sub>Cl nanocluster is stable enough and remains intact after loading on the pores of MSNs.

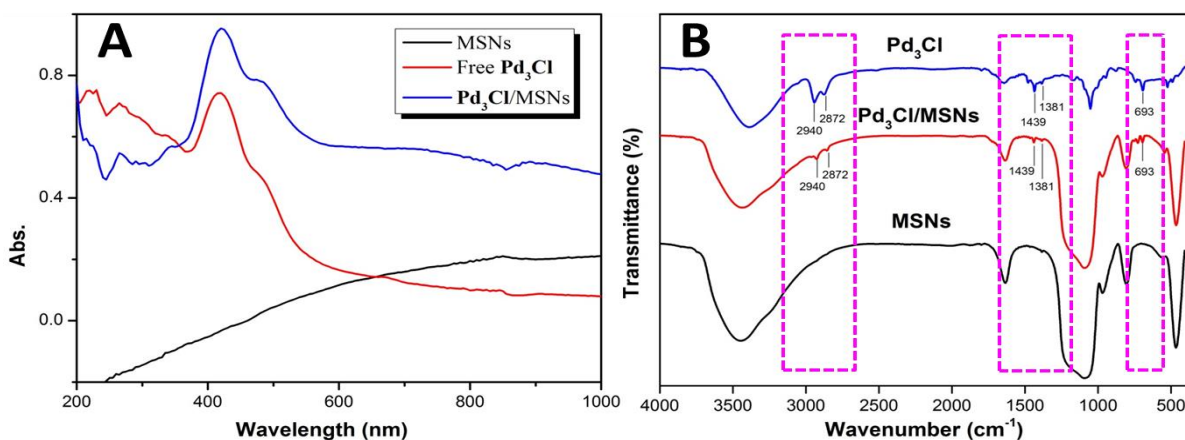


Fig. 3: (A) Diffuse reflectance optical spectra and (B) FT-IR spectra of MSNs, free Pd<sub>3</sub>Cl and Pd<sub>3</sub>Cl/MSNs.

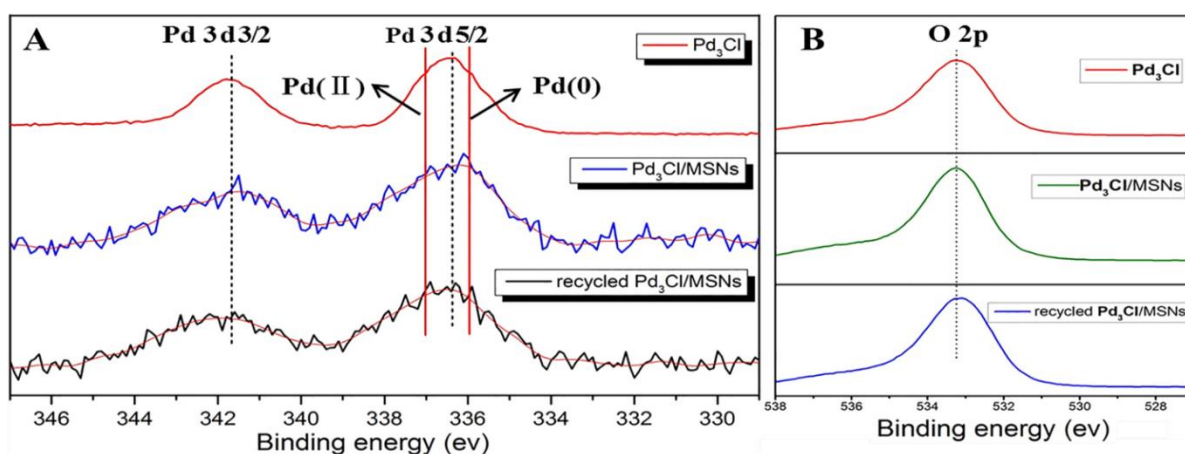


Fig. 4: XPS spectra in Pd 3d (A) and O 1s (B) of free Pd<sub>3</sub>Cl, MSNs, fresh and recycled Pd<sub>3</sub>Cl/MSNs catalysts.

To gain insight into the catalytic mechanism and the oxidation state of palladium nanocluster immobilized on the pores of MSNs, the free Pd<sub>3</sub>Cl nanocluster, MSNs, fresh and recycled Pd<sub>3</sub>Cl/MSNs were analyzed by X-ray photoelectron spectra (XPS). As shown in figure 4A, there are two observable peaks centred at 336.4 and 341.7 eV, which are assigned to Pd 3d<sub>5/2</sub> and Pd 3d<sub>3/2</sub>, respectively. In comparison of the standard binding energy of Pd(0) 3d<sub>5/2</sub> (~335.9 eV) and Pd(II) 3d<sub>5/2</sub> (~337.0 eV), we can conclude that the oxidation state of Pd in Pd<sub>3</sub>Cl nanocluster is between zero and two. The distinctive oxidation state of Pd in palladium nanocluster may play an important role in the alcohols oxidation reactions. After immobilized on the MSNs, the binding energy of Pd 3d has no obvious change. Similarly, the binding energy of O 2p of MSNs, in figure 4B, also remains unchanged.

Next, we investigated the catalytic performance of Pd<sub>3</sub>Cl/MSNs in the alcohols oxidation reactions. Initially, the benzyl alcohol was chosen for preliminary test and optimization of the reaction parameters (Table 1). Unfortunately, no reaction occurred when toluene or DCM as solvents (Table 1, entries 1 and 2). The same results were obtained even though the reaction temperature was elevated to 50 °C (Table 1, entries 3 and 4). To our delight, the desired product can be obtained in polar solvent, such as ethanol (Table 1, entry 5). Hence, the strong polar solvent, water was chosen as the solvent, a significant improvement of yield was achieved though the substrate and product are poorly dissolved in water (Table 1, entry 6). Detailed optimization of solvent indicated that water is the best among toluene, EtOH, DCM, CH<sub>3</sub>CN and DMF (Table 1, entries 7 and 8). The hydrophobic effect may have played an

important role in accelerating the reaction process, but the detailed mechanism of water remains unclear at this stage. Better results were obtained when  $\text{Na}_2\text{CO}_3$  as base (Table 1, entries 9 and 10). We further tested other commonly used oxidants, moderate yield obtained when  $\text{H}_2\text{O}_2$  as oxidant and the TBHP failed to oxidize the alcohol. When air acts as oxidizer, the oxidation reaction still carried out successfully, although the yield was unsatisfactory (Table 1, entries 11-13). The results of control experiment and blank experiment clearly suggest that the palladium nanocluster is the true catalytic species (Table 1, entries 13-14). Moreover, compared with commercially available heterogeneous catalyst (Pd/C),  $\text{Pd}_3\text{Cl}/\text{MSNs}$  shows higher catalytic activity under the optimized reaction conditions (Table 1, entry 16).

Table-1: Optimization of the reaction conditions<sup>a</sup>

Entry	Solvent	Base	T (°C)	Yield (%) <sup>b</sup>
1	Toluene	$\text{NEt}_3$	rt	n.r.
2	DCM	$\text{NEt}_3$	rt	n.r.
3	Toluene	$\text{NEt}_3$	50	n.r.
4	DCM	$\text{NEt}_3$	50	n.r.
5	EtOH	$\text{NEt}_3$	rt	15
6	$\text{H}_2\text{O}$	$\text{NEt}_3$	rt	72
7	$\text{CH}_3\text{CN}$	$\text{NEt}_3$	rt	Trace
8	DMF	$\text{NEt}_3$	rt	n.r.
9	$\text{H}_2\text{O}$	$\text{Na}_2\text{CO}_3$	rt	90
10	$\text{H}_2\text{O}$	$\text{K}_2\text{CO}_3$	rt	82
11 <sup>c</sup>	$\text{H}_2\text{O}$	$\text{Na}_2\text{CO}_3$	50	25
12 <sup>d</sup>	$\text{H}_2\text{O}$	$\text{Na}_2\text{CO}_3$	50	n.r.
13 <sup>e</sup>	$\text{H}_2\text{O}$	$\text{Na}_2\text{CO}_3$	rt	37
14 <sup>f</sup>	$\text{H}_2\text{O}$	$\text{Na}_2\text{CO}_3$	rt	n.r.
15 <sup>g</sup>	$\text{H}_2\text{O}$	$\text{Na}_2\text{CO}_3$	rt	n.r.
16 <sup>h</sup>	$\text{H}_2\text{O}$	$\text{Na}_2\text{CO}_3$	rt	67

<sup>a</sup>Reaction conditions: benzyl alcohol (0.2 mmol), additive (0.3 mmol), solvent (1 ml), catalyst (15 mg) for 24 h. <sup>b</sup>Isolated yields. <sup>c</sup>The reaction was carried out with  $\text{H}_2\text{O}_2$  as oxidant. <sup>d</sup>The reaction was carried out with TBHP as oxidant. <sup>e</sup>The reaction was carried out with air as oxidant. <sup>f</sup>The reaction was carried out without  $\text{Pd}_3\text{Cl}/\text{MSNs}$  catalyst. <sup>g</sup>The reaction was carried out with bare MSNs. <sup>h</sup>The reaction was carried out with Pd/C as catalyst. TBHP = tert-Butyl hydroperoxide

After optimizing the reaction conditions, the generality of the alcohols oxidation was then tested and the results are summarized in table 2. Generally, all of the reactions proceeded smoothly to give the desired aldehydes with good yields. It was found that the electron effect of substituents play a very important role in the yields of this reactions. Alcohol with electron-donating substituents gave better yields than those with electron-withdrawing ones. For example, compared with 4-nitrobenzyl alcohol, 4-Methylbenzyl alcohol and 4-Methoxybenzyl alcohol gave the high yields (entry 7 vs entries 2 and

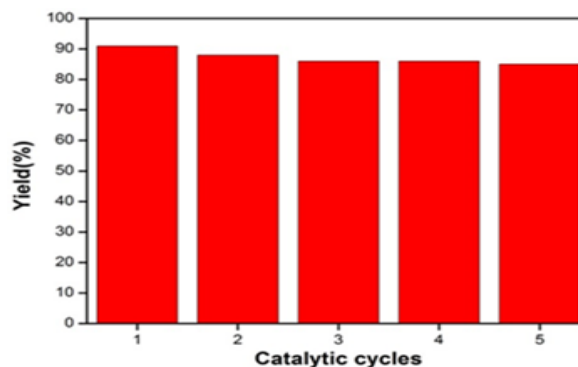
4). In addition, furfuryl alcohol could also be tolerated in this oxidation reaction, delivering the desired furfural in good yield (table 2, entry 12). Meanwhile,  $\alpha,\beta$ -unsaturated alcohol was also efficiently oxidized by the  $\text{Pd}_3\text{Cl}/\text{MSNs}$ .

Table-2: Substrate scope of the alcohols oxidation reactions<sup>a</sup>

Entry	R	Yield (%) <sup>b</sup>
1	Ph	88
2	4-MeOC <sub>6</sub> H <sub>4</sub>	94
3	3-MeOC <sub>6</sub> H <sub>4</sub>	92
4	4-MeC <sub>6</sub> H <sub>4</sub>	90
5	3-MeC <sub>6</sub> H <sub>4</sub>	89
6	2-MeC <sub>6</sub> H <sub>4</sub>	91
7	4-NO <sub>2</sub> C <sub>6</sub> H <sub>4</sub>	76
8	4-BrC <sub>6</sub> H <sub>4</sub>	81
9	3-BrC <sub>6</sub> H <sub>4</sub>	84
10	2-BrC <sub>6</sub> H <sub>4</sub>	87
11	4-CF <sub>3</sub> C <sub>6</sub> H <sub>4</sub>	80
12	2-Furyl	89
13	C <sub>6</sub> H <sub>5</sub> CH=CH	90

<sup>a</sup>Reaction conditions: alcohol (0.2 mmol),  $\text{Na}_2\text{CO}_3$  (0.3 mmol),  $\text{H}_2\text{O}$  (1 ml),  $\text{Pd}_3\text{Cl}/\text{MSNs}$  (15mg) for 24 h. <sup>b</sup>isolated yield.

Then, the reusability of the  $\text{Pd}_3\text{Cl}/\text{MSNs}$  catalysts was investigated. The  $\text{Pd}_3\text{Cl}/\text{MSNs}$  catalysts were recovered by centrifugation, washed with water and ethanol, and dried. A fresh reaction was run under identical conditions using the recycled catalyst. Indeed, the recycled catalyst showed almost as the same activity as the fresh catalyst after five catalytic cycles (Figure 5). In addition, the TEM image of recycled  $\text{Pd}_3\text{Cl}/\text{MSNs}$  indicated that the  $\text{Pd}_3\text{Cl}$  nanoclusters did not aggregate and the MSNs still maintain the original morphology after five catalytic cycles (Figure 6). The same conclusion could be obtained from the results of XPS data of recycled  $\text{Pd}_3\text{Cl}/\text{MSNs}$  (Figure 4). The excellent recyclability makes the  $\text{Pd}_3\text{Cl}/\text{MSNs}$  have great development potential in the industrial application.

Fig. 5: The recyclability of  $\text{Pd}_3\text{Cl}/\text{MSNs}$ .

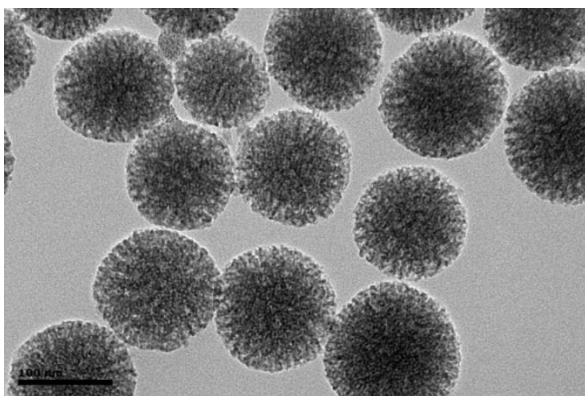


Fig. 6: The TEM image of Pd<sub>3</sub>Cl/MSNs after five catalytic cycles.

### Conclusion

In summary, the Pd<sub>3</sub>Cl/MSNs catalysts were successfully prepared via a simply impregnation method and well characterized by UV-vis, TEM, diffuse reflectance optical spectrum, FT-IR and XPS. The Pd<sub>3</sub>Cl/MSNs catalysts show excellent catalytic performance in aerobic oxidation of alcohols under extremely mild reaction conditions. Moreover, the Pd<sub>3</sub>Cl/MSNs catalysts can be easily reused without loss of its catalytic activity and the large-scale synthesis of cinnamyl aldehyde is also efficient. Further applications of this chemistry toward novel reaction design and synthesis of complex molecules are currently underway.

### Acknowledgement

We are grateful to the Shandong Province Natural Science Foundation (ZR2018PB003).

### References

- (a) U. M. Lindström, *Chem. Rev.*, **102**, 2751 (2002); (b) A. Chanda and V. V. Fokin, *Chem. Rev.*, **109**, 725 (2009); (c) R. N. Butler and A. G. Coyne, *Chem. Rev.*, **110**, 6302 (2010); (d) M.-O. Simon and C.-J. Li, *Chem. Soc. Rev.*, **41**, 1415 (2012); (e) M. B. Gawande, V. D. B. Bonifácio, R. Luque, P. S. Branco and R. S. Varma, *Chem. Soc. Rev.*, **42**, 5522 (2013); (f) F. Zhang and H. Li, *Chem. Sci.*, **5**, 3695 (2014); (g) T. Kitanosono, K. Masuda, P. Xu and S. Kobayashi, *Chem. Rev.*, **118**, 679 (2018).
- (a) A. S. Sharma, H. Kaur and D. Shah, *RSC Adv.*, **6**, 28688 (2016); (b) R. Ciriminna, V. Pandarus, F. Béland, Y.-J. Xu and M. Pagliaro, *Org. Process Res. Dev.*, **19**, 1554 (2015); (c) C. Xu, C. Zhang, H. Li, X. Zhao, L. Song and X. Li, *Catalysis Surveys from Asia*, **20**, 13 (2015); (d) A. M. Faisca Phillips, A. J. L. Pombeiro and M. N. Kopylovich, *ChemCatChem*, **9**, 217 (2017); (e) C. Parmeggiani, C. Matassini and F. Cardona, *Green Chem.*, **19**, 2030 (2017); (f) R. H. Crabtree, *Chem. Rev.*, **117**, 9228 (2017); (g) J. Liu, S. Wu and Z. Li, *Curr. Opin. Chem. Biol.*, **43**, 77 (2018); (h) F. Liu, H. Wang, A. Sapi, H. Tatsumi, D. Zhrebetsky, H.-L. Han, L. Carl and G. Somorjai, *Catalysts*, **8**, 226 (2018); (i) C. Chan-Thaw, A. Savara and A. Villa, *Catalysts*, **8**, 431 (2018).
- (a) F. Vindigni, S. Dughera, F. Armigliato and A. Chiorino, *Monatsh für Chemie-Chemical Monthly*, **147**, 391 (2015); (b) Y. Li, Y. Gao and C. Yang, *Chem. Commun.*, **51**, 7721 (2015).
- Y.-M. Lu, H.-Z. Zhu, J.-W. Liu, S.-H. Yu, *ChemCatChem*, **7**, 4131 (2015).
- H. Liu, L. Chang, C. Bai, L. Chen, R. Luque and Y. Li, *Angew. Chem. Int. Ed.*, **55**, 5019 (2016).
- (a) A. Saha, S. Payra and S. Banerjee, *New J. Chem.*, **41**, 13377 (2017); (b) H. Liu, D. Ramella, P. Yu and Y. Luan, *RSC Adv.*, **7**, 22353 (2017); (c) Y. Qi, Y. Luan, J. Yu, X. Peng and G. Wang, *Chemistry*, **21**, 1589 (2015); (d) H. Sand and R. Weberskirch, *Polym. Int.*, **66**, 428 (2017); (e) B. R. Kim, J. S. Oh, J. Kim and C. Y. Lee, *Catal. Lett.*, **146**, 734 (2016); (f) L. Marais, J. Bures, J. H. L. Jordaan, S. Mapolie and A. J. Swarts, *Org. Biomol. Chem.*, **15**, 6926 (2017).
- S. Ji, Y. Chen, Q. Fu, Y. Chen, J. Dong, W. Chen, Z. Li, Y. Wang, L. Gu, W. He, C. Chen, Q. Peng, Y. Huang, X. Duan, D. Wang, C. Draxl and Y. Li, *J. Am. Chem. Soc.*, **139**, 9795 (2017).
- (a) A. DeViernoKreuder, T. House-Knight, J. Whitford, E. Ponnusamy, P. Miller, N. Jesse, R. Rodenborn, S. Sayag, M. Gebel, I. Aped, I. Sharfstein, E. Manaster, I. Ergaz, A. Harris and L. Nelowet Grice, *ACS Sustainable Chem. Eng.*, **5**, 2927 (2017); (b) H. C. Erythropel, J. B. Zimmerman, T. M. de Winter, L. Petitjean, F. Melnikov, C. H. Lam, A. W. Lounsbury, K. E. Mellor, N. Z. Janković, Q. Tu, L. N. Pincus, M. M. Falinski, W. Shi, P. Coish, D. L. Plata and P. T. Anastas, *Green Chem.*, **20**, 1929 (2018).
- (a) R. Jin, *Nanoscale*, **2**, 343 (2010); (b) Y. Lu and W. Chen, *Chem. Soc. Rev.*, **41**, 3594 (2012); (c) B. H. Kim, M. J. Hackett, J. Park and T. Hyeon, *Chem. Mater.*, **26**, 59 (2013); (d) H. Qian, M. Zhu, Z. Wu and R. Jin, *Acc. Chem. Res.*, **45**,

- 1470 (2012); (e) L. Cademartiri and V. Kitaev, *Nanoscale*, **3**, 3435 (2011); (f) R. Jin, C. Zeng, M. Zhou and Y. Chen, *Chem. Rev.*, **116**, 10346 (2016); (g) I. Chakraborty and T. Pradeep, *Chem. Rev.*, **117**, 8208 (2017).
10. S. Yamazoe, K. Koyasu and T. Tsukuda, *Acc. Chem. Res.*, **47**, 816(2014).
11. (a) Y. Zhu, H. Qian, B. A. Drake and R. Jin, *Angew. Chem. Int. Ed.*, **49**, 1295 (2010); (b) G. Li and R. Jin, *J. Am. Chem. Soc.*, **136**, 11347 (2014); (c) G. Li, H. Abroshan, Y. Chen, R. Jin and H. J. Kim, *J. Am. Chem. Soc.*, **137**, 14295 (2015).
12. (a) H. Abroshan, G. Li, J. Lin, H. J. Kim and R. Jin, *J. Catal.*, **337**, 72 (2016); (b) G. Li, H. Abroshan, C. Liu, S. Zhuo, Z. Li, Y. Xie, H. J. Kim, N. L. Rosi and R. Jin, *ACS Nano*, **10**, 7998 (2016); (c) G. Li, C. Liu, Y. Lei and R. Jin, *Chem. Commun.*, **48**, 12005 (2012).
13. (a) Y. Du, H. Sheng, D. Astruc and M. Zhu, *Chem. Rev.*, **120**, 526 (2020); (b) G. Li and R. Jin, *Acc. Chem. Res.*, **46**, 1749 (2013); (c) Y. Zhu, R. Jin and Y. Sun, *Catalysts*, **1**, 3 (2011); (d) Y. Zhu, H. Qian and R. Jin, *J. Mater. Chem.*, **21**, 6793 (2011); (e) J. Zhao and R. Jin, *Nano Today*, **18**, 86 (2018); (f) J. Fang, B. Zhang, Q. Yao, Y. Yang, J. Xie and N. Yan, *Coord. Chem. Rev.*, **322**, 1 (2016).
14. S. Xie, H. Tsunoyama, W. Kurashige, Y. Negishi and T. Tsukuda, *ACS Catal.*, **2**, 1519 (2012).
15. F. Fu, J. Xiang, H. Cheng, L. Cheng, H. Chong, S. Wang, P. Li, S. Wei, M. Zhu and Y. Li, *ACS Catal.*, **7**, 1860 (2017).
16. Y. Yun, H. Sheng, J. Yu, L. Bao, Y. Du, F. Xu, H. Yu, P. Li and M. Zhu, *Adv. Synth. Catal.*, **360**, 4731(2018)